Published in final edited form as:
J Magn Reson. 2011 April ; 209(2): 131–135. doi:10.1016/j.jmr.2010.12.011.

Straightforward, effective calibration of SPINAL-64 decoupling results in the enhancement of sensitivity and resolution of biomolecular solid-state NMR

Gemma Comellas[§], **Jakob J. Lopez**[‡], **Andrew J. Nieuwkoop**[‡], **Luisel R. Lemkau**[‡], and **Chad M. Rienstra**[††,§,‡,‖]

[§]Center for Biophysics and Computational Biology, University of Illinois at Urbana-Champaign, 600 South Mathews Avenue, Urbana, Illinois 61801

[‡]Department of Chemistry, University of Illinois at Urbana-Champaign, 600 South Mathews Avenue, Urbana, Illinois 61801

[‖]Department of Biochemistry, University of Illinois at Urbana-Champaign, 600 South Mathews Avenue, Urbana, Illinois 61801

Abstract

We describe a simple yet highly effective optimization strategy for SPINAL-64 ^{1}H decoupling conditions for magic-angle spinning solid-state NMR. With adjustment of the phase angles in a coupled manner, the optimal conditions resulting from three parameter optimizations can be determined with adjustment of a single phase. Notably, echo T_2 relaxation times for ^{13}C and ^{15}N show significant enhancement (up to 64%), relative to the previous described SPINAL-64 conditions, under the moderate ^{1}H decoupling levels (60 – 100 kHz) and MAS rate (13.3 kHz) commonly employed for high-resolution SSNMR spectroscopy of proteins. Additionally, we also investigated the effect at higher spinning rate (33.3 kHz) and compared the results with other ^{1}H decoupling schemes (TPPM, XiX), as well as SPINAL-64 with the originally reported optimal values.

Keywords

magic-angle spinning; solid-state MMR; proton decoupling; SPINAL-64

1. Introduction

High-resolution spectra are essential for the study of large biological systems by magic-angle spinning (MAS) solid-state NMR (SSNMR) spectroscopy. One of the main limitations for such studies are imposed by the lifetimes of transverse magnetization (T_2) [1] for the observed nuclei, due to the strong dipolar coupling interactions between ^{1}H and X (usually ^{13}C or ^{15}N) [2]. As a result, considerable research effort has resulted in a plethora of ^{1}H decoupling sequences[3–6].

[††]Corresponding author information: Chad M. Rienstra, Department of Chemistry, University of Illinois at Urbana-Champaign, 600 South Mathews Avenue, Urbana, IL 61801, USA. Telephone: (+01) 217 244-4655. Fax: 217 244-3186. rienstra@scs.illinois.edu.

Continuous-wave (CW) [7] decoupling was for many years the only effective heteronuclear ^{1}H method for rigid solids, but for most applications has been supplanted by two pulse phase-modulation (TPPM) [8], which consists of a series of near π pulses with alternating phases (see Fig. 1b). A variety of ^{1}H decoupling methods with phase and/or frequency modulations extending upon the TPPM approach were subsequently developed [3–6]. Among these, we have observed that SPINAL-64 (small phase incremental alternation with 64 steps, Fig. 1b) [9], is particularly robust with respect to radio-frequency (RF) inhomogeneity and/or pulse width imperfection and has better compensation for resonance offsets, arising from the compensatory super cycles of the basic SPINAL element. SPINAL-64 has also been described to be superior in performance under some regimes of decoupling power than TPPM [10]. The benefits of SPINAL are particularly evident, in comparison with CW decoupling, for magnetically aligned samples [11].

In the original publication describing SPINAL-64, Fung *et al.* note the optimal values for the flip angle θ, phase angle ϕ, and phase increments α and β to be, 11/12 π, 10°, 5° and 10° [9], respectively. Thakur *et al*. reported improvements in performance and efficiency upon modification of the phase (from 1 to 5°) and angle increments (from 3–16°) on crystalline glycine [12]. In the course of utilizing the SPINAL-64 sequence for studies of biomolecular samples including nanocrystalline, fibrillar and membrane proteins, at different moderate MAS rates (10–16.7 kHz), we found that different phase angles from the ones previously reported were consistently preferred. Although we arrived at these values by empirical, experimental optimization in three dimensions, we have also identified trends that enable the global optimum solution to be found in a small fraction of the total optimization time. The results yield an improved decoupling performance, as shown in Figure 1 for N-acetyl valine (NAV). The changes in phase parameters are modest, but yield substantial benefits in relaxation times and resolution for 2D MAS NMR spectra.

2. Results and discussion

A comparison of the ^{13}C and ^{15}N transverse magnetization lifetimes (T_2) for the originally reported optimal values [9] and the values we obtain on our samples following optimization is depicted in Figure 2. An increase for the T_2 values up to 64% (^{15}N) and 25% (^{13}C) were noted for uniformly ^{13}C-^{15}N enriched A30P alpha-synuclein (AS) in fibrillar form (Figure 2). A comparison of two frequently used 2D correlation experiments is depicted in Figure 3, using the originally reported optimal values [9] (left) and the optimized values (right), with a ^{1}H decoupling power of 80 kHz. These spectra (^{13}C-^{13}C with 50 ms DARR mixing and ^{15}N-^{13}C with specific CP) demonstrate an improved sensitivity (up to 80% enhancement of the S/N or 125% of the peak height for Ala CA-CB cross-peaks and 63% of the S/N or 100% of the peak height for Thr CA-CB cross-peaks) and linewidths (up to 67% for the ^{15}N and 44% for ^{13}C in the $^{15}N^{13}CA$ 2D), as shown in expanded regions in Figure 3.

We optimized SPINAL-64 ^{1}H decoupling with respect to the flip angle (θ), the phase angle (ϕ) and the phase increments α and β (see arrays in Figure 4 for A30P AS fibrils). During optimization, θ was varied from 150° to 210°, ϕ from 0° to 10°, and α from 0° to 10°. These optimizations, conducted on a variety of biological samples, demonstrated that the best values, under the moderate ^{1}H decoupling levels and MAS rate commonly employed for high-resolution SSNMR, occur when the parameters φ and α add up to 10° (as shown for A30P AS fibrils and NAV in Tables 1 and 2, respectively), which corresponds to arrays located in the diagonal of the plots (indicated with darker background in Figure 1 and 4). Thus, the most efficient optimization of SPINAL-64 would include a 3D array of θ, ϕ from 0° to 10° and α from 10° to 0°, where ϕ and α add to 10° in each step in a single dimension of the array. In all these experiments the variable parameter β was set to two times α, which corresponds to the optimum or very close to the optimum, as shown in Figure 4.

The improvement of transversal magnetization lifetimes of ^{13}C and ^{15}N is clearly shown using NAV (Figure 2), but also demonstrates an improvement of SPINAL-64 versus TPPM or XiX, when the variable parameters are optimized at a moderate MAS rate (13.3) and commonly employed power levels (70–100 kHz) for high-resolution SSNMR [10] (see Figure 1). In the optimization arrays, θ was varied from 150° to 210° for SPINAL-64 and TPPM, ϕ from 0° to 10° and α from 0° to 10° for SPINAL-64 and ϕ from 0° to 30° for TPPM. These arrays also demonstrate a smaller dependence of the signal intensity on the decoupling pulse duration for SPINAL-64 and thus more experimental stability with respect to changes in pulse widths for a selected conditions than TPPM over the same range of θ and ϕ, which is an important requirement for conducting long multidimensional experiments in biomolecular SSNMR.

Finally, we also explored the effect of the optimization at a higher MAS rate (33.333 kHz), as reported on Tables 2–4. Our results demonstrate a considerable improvement in the performance of SPINAL-64 over the originally optimal reported [9] variable parameters and shows that SPINAL-64 with the optimized parameters behaves similarly or better than TPPM or XiX for ^{1}H decoupling powers between 70–100 kHz. At high MAS rate (33.333 kHz), the optimization arrays showed slightly different preferred values for the variable parameters than observed for moderate spinning rates. The best values occur when the parameters φ and α add up to 8° and/or 10°, depending on the power level.

3. Conclusions

By optimizing the variable parameters for SPINAL-64 ^{1}H decoupling for a variety of biological samples, we observed a considerable improvement in the performance of SPINAL-64 versus the originally reported parameters (θ=(11/12)π, φ= 10°, α=5° and β=10°) [9]. Here, we have reported a series of experiments to demonstrate the effect on the T_2s for A30P AS fibrils and NAV at different power levels, as a comparison with the originally reported values, TPPM and XiX decoupling, as well as the effect in multidimensional SSNMR experiments. Our results show an improvement up to 64 % in the T_2s and a sensitivity enhancement up to 80% of S/N of individual peaks in multidimensional experiments of A30P AS fibrils that lead to significant improvement in the spectra resolution.

4. Experimental

U-^{13}C,^{15}N-labeled A30P AS was prepared as described in Kloepper *et. al.* [13] and fibrils were prepared for SSNMR as recent studies for the wild-type AS fibrils describe elsewhere. Samples were packed into 1.6 and 3.2 mm MAS NMR rotors (Varian, Inc., Palo Alto, CA) and confined to the active sample region of the rotor and kept hydrated by Kel-F and rubber spacers [14].

All experiments were carried out with the variable temperature gas at 10 °C, which corresponded to an actual sample temperature of 14 °C, as determined by ethylene glycol calibration [15]. Experiments were carried out on a 600 MHz Infinity Plus spectrometer (Varian NMR) equipped with a HXY (T3) probe tuned to ^{1}H-^{13}C-^{15}N triple mode at 13.333 kHz MAS rate and on a 750 MHz Wide Bore Vnmrs spectrometer (Varian NMR) equipped with a HFXY probe tuned to ^{1}H-^{13}C-^{15}N triple mode at 13.333 and 33.333 kHz MAS rates. For the 600 MHz spectrometer, the NAV π/2 pulse widths for ^{1}H and ^{13}C were 1.90 and 2.70 μs, respectively, and for A30P AS fibrils, the π /2 pulse widths for ^{1}H, ^{13}C, ^{15}N were 2.25, 2.62 and 3.75 μs, respectively. For the 750 MHz spectrometer, the NAV π/2 pulse widths for ^{1}H, ^{13}C and ^{15}N were 1.90, 2.20 and 3.90 μs, respectively. All experiments utilized tangent ramped cross polarization [16]. TPPM [8], SPINAL-64 [9] and XiX [9] ^{1}H

decoupling was applied during acquisition and evolution periods. For the 2D ^{13}C-^{13}C spectra, the dipolar assisted rotational resonance (DARR) scheme [17] was used for ^{13}C-^{13}C mixing. For the 2D NCA experiments, a selective SPECIFIC CP [18] was used for polarization transfer from ^{15}N to ^{13}C. Average echo T_2s (typically referred to as T_2' [1]) values for ^{13}CA and ^{15}N at different decoupling conditions and optimization conditions were measured using a 1D CP Hahn-echo [19]experiment with a 180° soft pulse on ^{15}CA resonance to remove the effect of ^{13}C-^{13}C *J*-couplings [20] (no soft pulse was used for the ^{15}N measurement). Chemical shifts were referenced externally with adamantane (assuming the downfield peak to resonate at 40.48 ppm) [21].

Plotting and data analysis were carried out with scripts written in house, using Python 2.5, specifically with the python modules `scipy' and `matplotlib'. 2D spectra were processed with NMRPipe [22] and were analyzed with Sparky program[23]. Back linear prediction and polynomial baseline correction were applied to the direct dimension. Zero filling and Lorentzian-to-Gaussian apodization were used for each dimensions before Fourier transformation.

Supplementary Material

Refer to Web version on PubMed Central for supplementary material.

Acknowledgments

This work was supported by the National Institutes of Health (R01-GM073770 and R01-GM073770 ARRA supplement to C.M.R.). The authors would like to thank Dr. Ming Tang for carefully reading the manuscript.

References

[1]. Lesage A, Bardet M, Emsley L. Through-bond carbon-carbon connectivities in disordered solids by NMR. J. Am. Chem. Soc. 1999; 121:10987–10993.

[2]. Ernst M. Heteronuclear spin decoupling in solid-state NMR under magic-angle sample spinning. J. Magn. Reson. 2003; 162:1–34. [PubMed: 12762980]

[3]. Gan Z, Ernst RR. Frequency- and phase-modulated heteronuclear decoupling in rotating solids. Solid State Nucl. Magn. Reson. 1997; 8:153–159. [PubMed: 9211619]

[4]. Detken A, Hardy EH, Ernst M, Meier BH. Simple and efficient decoupling in magic-angle spinning solid- state NMR: the XiX scheme. Chem. Phys. Lett. 2002; 356:298–304.

[5]. Takegoshi K, Mizokami J, Terao T. H-1 decoupling with third averaging in solid NMR. Chem. Phys. Lett. 2001; 341:540–544.

[6]. Weingarth M, Bodenhausen G, Tekely P. Low-power decoupling at high spinning frequencies in high static fields. J. Magn. Reson. 2009; 199:238–241. [PubMed: 19467891]

[7]. Haeberlen U, Waugh A. Coherent Averaging Effect in Magnetic Resonance. Phys. Rev. 1968; 175:453–467.

[8]. Bennett AE, Rienstra CM, Auger M, Lakshmi KV, Griffin RG. Heteronuclear decoupling in rotating solids. J. Chem. Phys. 1995; 103:6951–6958.

[9]. Fung BM, Khitrin AK, Ermolaev K. An improved broadband decoupling sequence for liquid crystals and solids. J. Magn. Reson. 2000; 142:97–101. [PubMed: 10617439]

[10]. Brauniger T, Wormald P, Hodgkinson P. Improved proton decoupling in NMR spectroscopy of crystalline solids using the SPINAL-64 sequence. Monatshefte Fur Chemie. 2002; 133:1549–1554.

[11]. Sinha N, Grant CV, Wu CH, De Angelis AA, Howell SC, Opella SJ. SPINAL modulated decoupling in high field double- and triple-resonance solid-state NMR experiments on stationary samples. J. Magn. Reson. 2005; 177:197–202. [PubMed: 16137902]

[12]. Thakur RS, Kurur ND, Madhu PK. An analysis of phase-modulated heternuclear dipolar decoupling sequences in solid-state nuclear magnetic resonance. J. Magn. Reson. 2008; 193:77–88. [PubMed: 18457968]

[13]. Kloepper KD, Woods WS, Winter KA, George JM, Rienstra CM. Preparation of alpha-synuclein fibrils for solid-state NMR: Expression, purification, and incubation of wild-type and mutant forms. Protein Expression Purif. 2006; 48:112–117.

[14]. Franks WT, Zhou DH, Wylie BJ, Money BG, Graesser DT, Frericks HL, Sahota G, Rienstra CM. Magic-angle spinning solid-state NMR spectroscopy of the beta-1 immunoglobulin binding domain of protein G (GB1): ^{15}N and ^{13}C chemical shift assignments and conformational analysis. J. Am. Chem. Soc. 2005; 127:12291–12305. [PubMed: 16131207]

[15]. Van Geet AL. Calibration of the methanol and glycol nuclear magnetic resonance thermometers with a static thermistor probe. Anal. Chem. Anal. Chem. 1968; 42:2227–2229.

[16]. Hediger S, Meier BH, Kurur ND, Bodenhausen G, Ernst RR. NMR cross-polarization by adiabatic passage through the Hartmann-Hahn condition (APHH). Chem. Phys. Lett. 1994; 223:283–288.

[17]. Takegoshi K, Nakamura S, Terao T. C-13-H-1 dipolar-assisted rotational resonance in magic-angle spinning NMR. Chem. Phys. Lett. 2001; 344:631–637.

[18]. Baldus M, Petkova AT, Herzfeld J, Griffin RG. Cross polarization in the tilted frame: assignment and spectral simplification in heteronuclear spin systems. Mol. Phys. 1998; 95:1197–1207.

[19]. Hahn EL. Spin Echoes. Phys. Rev. 1950; 80:580–594.

[20]. Li Y, Wylie BJ, Rienstra CM. Selective refocusing pulses in magic-angle spinning NMR: Characterization and applications to multi-dimensional protein spectroscopy. J. Magn. Reson. 2006; 179:206–216. [PubMed: 16406627]

[21]. Morcombe CR, Zilm KW. Chemical shift referencing in MAS solid state NMR. J. Magn. Reson. 2003; 162:479–486. [PubMed: 12810033]

[22]. Delaglio F, Grzesiek S, Vuister GW, Zhu G, Pfeifer J, Bax A. Nmrpipe: a Multidimensional Spectral Processing System Based On Unix Pipes. J. Biomol. NMR. 1995; 6:277–293. [PubMed: 8520220]

[23]. Goddard, TD.; Kneller, DG. Sparky 3. University of California; San Francisco: 2006.

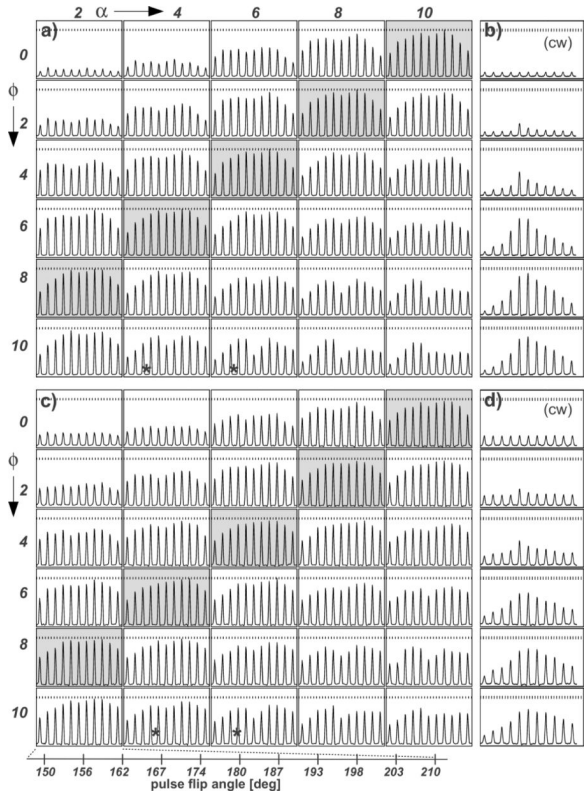

Fig. 1.

Part of the arrays of the variable parameters for ^{13}C detection with (a) SPINAL-64 and (b) TPPM and ^{15}N detection with (c) SPINAL-64 and (d) TPPM ^{1}H decoupling for NAV. All arrays were acquired with 85 kHz of decoupling power at 750 MHz ^{1}H frequency and 13.3 kHz MAS. A soft pulse was used to select the ^{13}CA. Spectra labeled with (*) correspond to the closed conditions to the optimal reported values ($\theta=(11/12)\pi$, $\varphi= 10°$, $\alpha=5°$ and $\beta=10°$) [9]. Horizontal dashed lines correspond to the highest peak height level obtained from the optimized conditions.

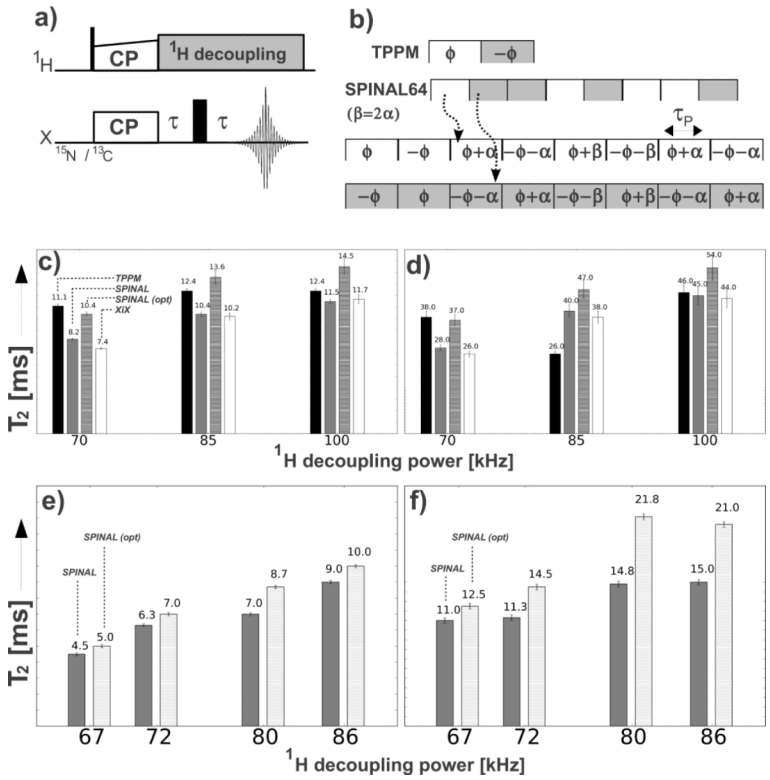

Fig. 2.

Schematic representation of (a) the pulse sequence used for the determination of the T_2 values with (b) TPPM and SPINAL-64 ^{1}H decoupling (flip angle (θ), phase angle (ϕ) and phase increments α and β for the phase angle). Comparison of T_2 values between TPPM, SPINAL-64 with the optimal reported values (θ =(11/12)π, φ= 10°, α=5° and β=10°) [9] and the optimized parameters (opt.) and XiX for NAV at different ^{1}H decoupling powers (70, 85, 100 kHz) for (c) ^{13}C detection and (d) ^{15}N detection. All arrays were acquired at 13.3 kHz MAS and 750 MHz ^{1}H frequency. Comparison of T_2 values between SPINAL-64 with the optimal reported values (θ =(11/12)π, φ= 10°, α=5° and β=10°) [9] and the optimized parameters for A30P AS fibrils at different ^{1}H decoupling powers (67, 72, 80, 85 kHz) for (e) ^{13}C detection and (f) ^{15}N detection at 13.3 kHz and 600 MHz. Error bars correspond to the error associated with the fitting of the experimental data.

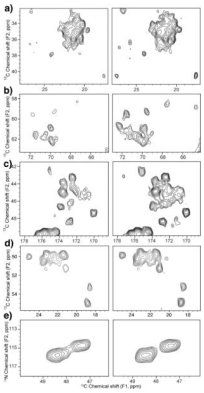

Fig. 3.

Comparison of expanded regions of A30P AS fibrils 2D spectra acquired with (left) optimal reported values (θ =(11/12)π, φ= 10°, α=5° and β=10°) [9] and (right) optimized values of the SPINAL-64 ^{1}H decoupling (80 kHz) for a ^{13}C^{13}C spectrum with 50 ms DARR mixing time: (a) methyl region (b) Thr and Ser CA-CB, (c) Gly CA-C and (d) Ala CA-CB correlations and (e) ^{15}N^{13}CA spectrum with some Gly correlations. Both spectra were acquired under identical conditions at 600 MHz (^{1}H frequency) and 13.333 kHz MAS rate. Contour levels were draw at 7 σ. Full spectra are shown in Figure S1.

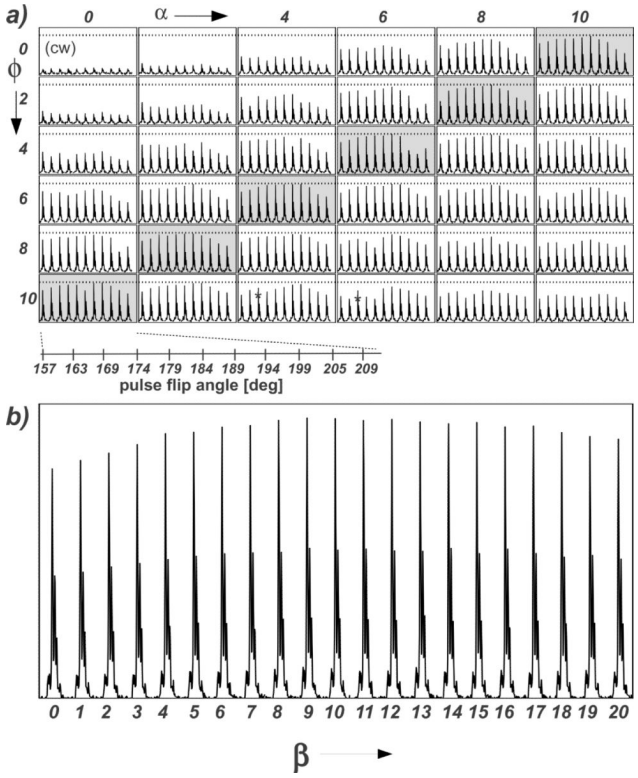

Fig. 4.

(a) Array of the SPINAL-64 parameters (θ, φ and α; β=2α) for A30P AS fibrils at 80 kHz ^{1}H decoupling for ^{13}C detection. Soft pulses were used to select the ^{13}CA. Spectra labeled with (*) correspond to the closed conditions to the optimal reported values (θ =(11/12)π, φ= 10°, α=5° and β=10°) [9]. Horizontal dashed lines correspond to the highest peak height level obtained from the optimized conditions. (b) Array of the SPINAL-64 parameter β (from 0 to 20, in steps of 1) for A30P AS fibrils at 80 kHz (θ =184°, φ= 6°, α=4°) with ^{13}C detection and soft pulse to select the ^{13}CA).

Table 1

Optimized parameters for SPINAL-64 ^{1}H decoupling for A30P AS fibrils at different ^{1}H decoupling power levels with ^{13}C and ^{15}N detection acquired at 13.3 kHz MAS and 600 MHz ^{1}H frequency.

Power (kHz)	SPINAL-64 parameters							
	^{13}C detection				^{15}N detection			
	θ (°)	φ (°)	α (°)	β (°)	θ (°)	φ (°)	α (°)	β (°)
67	178	6	4	8	180	4	8	16
73	188	8	2	4	188	4	6	12
80	184	6	4	8	179	4	6	12
86	174	4	6	12	174	8	2	4

Table 2

Optimized parameters for SPINAL-64 ^{1}H decoupling for NAV at different ^{1}H decoupling power levels (70–100 kHz) and MAS rates (13.3 – 33.3 kHz) MAS for ^{13}C and ^{15}N detection acquired at 750 MHz ^{1}H frequency.

MAS (Hz)	Power (kHz)	SPINAL-64 parameters							
		^{13}C detection				^{15}N detection			
		θ (°)	φ (°)	α (°)	β (°)	θ (°)	φ (°)	α (°)	β (°)
13333	70	195	8	2	4	198	6	4	8
	85	192	6	4	8	199	6	4	8
	100	195	6	4	8	190	8	2	4
33333	70	169	6	2	4	169	6	2	4
	85	186	6	2	4	186	6	4	8

Table 3

^{13}CA T_2 values for N-acetylvaline (NAV) at different ^{1}H decoupling power levels (70–100 kHz) and schemes (TPPM, SPINAL-64 with originally reported optimal [9] and optimized variable parameters and XiX) at 750 MHz ^{1}H frequency. ^{1}H carrier was set at the frequency of the ^{1}HA peak. Error bars correspond to the error associated with the fitting.

MAS (Hz)	Power (kHz)	^{13}CA T_2 (ms)			
		TPPM	SPINAL-64 (original variable parameters)	SPINAL-64 (optimized variable parameters)	XiX
13333	70	11.1 ± 0.2	8.2 ± 0.1	10.4 ± 0.2	7.4 ± 0.1
	85	12.4 ± 0.2	10.4 ± 0.2	13.6 ± 0.6	10.2 ± 0.3
	100	12.4 ± 0.2	11.5 ± 0.2	14.5 ±0.7	11.7 ± 0.4
33333	70	3.0 ± 0.1	1.2 ± 0.1	5.8 ± 0.1	3.7 ± 0.1
	85	8.8 ± 0.1	2.1 ± 0.1	9.6 ± 0.1	10.5 ± 0.1

Table 4

^{15}N T_2 measurements for N-acetylvaline (NAV) at different ^{1}H decoupling power levels and schemes (TPPM, SPINAL-64 with originally reported optimal [9] and optimized variable parameters and XiX). ^{1}H carrier was set at the frequency of the ^{1}HN peak. Error bars correspond to the error associated with the fitting.

MAS (Hz)	Power (kHz)	^{15}N T_2 (ms)			
		TPPM	SPINAL-64 (original variable parameters)	SPINAL-64 (optimized variable parameters)	XiX
13333	70	38 ± 2	28 ± 1	37 ± 2	26 ± 1
	85	26 ± 1	40 ± 2	47 ± 3	38 ± 2
	100	46 ± 3	45 ± 3	54 ± 4	44 ± 3
33333	70	8.0 ± 0.4	2.5 ± 0.2	7.3 ± 0.5	3.7 ± 0.1
	85	20.2 ± 0.6	7.1 ± 0.4	20.0 ± 0.9	12.8 ± 0.1